PHILOSOPHICAL TRANSACTIONS OF THE ROYAL SOCIETY A MATHEMATICAL, PHYSICAL & ENGINEERING SCIENCES

The Remanent Magnetic Field of the Moon

P. J. Coleman and C. T. Russell

Phil. Trans. R. Soc. Lond. A 1977 **285**, 489-506
doi: 10.1098/rsta.1977.0093

Phil. Trans. R. Soc. Lond. A. **285**, 489–506 (1977) [489]
Printed in Great Britain

The remanent magnetic field of the Moon

By P. J. Coleman, Jr and C. T. Russell
Institute of Geophysics and Planetary Physics, University of California, Los Angeles, California 90024, *U.S.A.*

Introduction

This paper is intended as a review of the empirical data on the remanent magnetic field of the Moon. These data are from direct measurements of the remanent field with magnetometers on the lunar surface and on board the Apollo subsatellites, and indirect measurements derived from studies of the interactions of the solar wind and energetic particles with the Moon.

Measurements on the surface of the Moon

In a series of experiments performed during the Apollo program, Sonett, Dyal, and co-workers obtained measurements of the Moon's remanent magnetic field at the sites of Apollos 12, 14, 15 and 16. (Dyal *et al.* (1974) have recently reviewed this work.) Two types of vector magnetometers were used in these experiments: a fixed, or station instrument; and a portable, or traverse, unit.

The portable magnetometer provided measurements of the vector field at several locations in the vicinity of the landing sites of Apollos 14 and 16. The station magnetometer provided measurements of the vector field and its gradient, over a distance of the order of 1 m, at stations near the landing sites of Apollos 12, 15 and 16.

At the site of Apollo 14, two measurements were taken at points separated by 1.1 km. At the Apollo 16 site five measurements, including one obtained with a station magnetometer, were taken at locations separated by as much as 7.1 km. In the station magnetometer measurements at the sites of Apollos 12 and 15, there are altogether nine measurements of the field on the surface of the Moon. At these nine locations, the remanent magnetic field ranges in intensity from 3 to 330 nT. At the five locations near the landing site of Apollo 16, the range is 110–330 nT. The measurements are listed in table 1, taken from Dyal *et al.* (1973).

These same workers have estimated the scale size of the source regions at two of the sites. For the Apollo 12 site, they used the gradient measured with the station magnetometer and that measured between the station magnetometer and the lunar orbiting spacecraft, Explorer 35, to obtain an estimate of 2–200 km for the allowable range of scale size (Dyal *et al.* 1972). For the Apollo 16 site, they used the surface measurements and measurements from the orbiting Apollo subsatellites to obtain an allowable range of 5–100 km (Dyal *et al.* 1974).

Measurements from lunar orbit

The Moon's remanent field was also measured from lunar orbit with the Apollo subsatellites. These small lunar satellites were launched from the Apollo spacecraft during the missions of Apollos 15 and 16. The orbit of the Apollo 15 subsatellite was inclined at 29° to the Moon's

equatorial plane and its orbital altitude ranged from 60 to 170 km. Magnetic field measurements were recorded for an interval of seven months from launch date. The orbit of the Apollo 16 subsatellite was inclined at 10° and its orbital altitude ranged from 205 to 0 km. This unfortunate lower limit was reached only 35 days after the launch. Details of the subsatellites and their instrumentation are given in Coleman *et al.* (1972*a*).

TABLE 1. SUMMARY OF LUNAR SURFACE REMANENT MAGNETIC FIELD MEASUREMENTS
(after Dyal *et al.* 1973)

	mag.	up	east	north (nT)
Apollo 16, 8.9° S, 15.5° E				
Alsep site	235 ± 4	−186 ± 4	−48 ± 3	+135 ± 3
site 2	189 ± 5	−189 ± 5	+3 ± 6	+10 ± 3
site 5	112 ± 5	+104 ± 5	−5 ± 4	−40 ± 3
site 13	327 ± 7	−159 ± 6	−190 ± 8	−214 ± 6
L.R.U. final site	113 ± 4	−66 ± 4	−76 ± 4	+52 ± 2
Apollo 15, 26.1° N, 3.7° E				
Alsep site	3.4 ± 2.9	+3.3 ± 1.5	+0.9 ± 2.0	−0.2 ± 1.5
Apollo 14, 3.7° S, 17.5° W				
site A } 1.1 km apart	103 ± 5	−93 ± 4	+38 ± 5	+24 ± 5
site C′ } 1.1 km apart	43 ± 6	−15 ± 4	−36 ± 5	−19 ± 8
Apollo 12, 3.2° S, 23.4° W				
Alsep site	38 ± 2	−25.8 ± 1.0	+11.9 ± 0.9	−25.8 ± 0.4

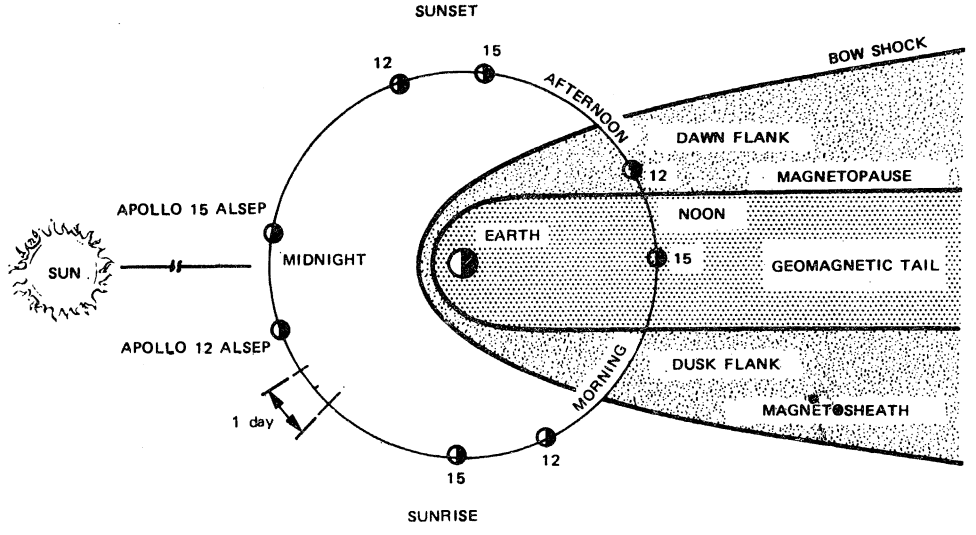

FIGURE 1. Schematic cross sectional diagram of the three environmental regimes through which the Moon passes in its orbit around the Earth. The view is from the ecliptic north pole.

Figure 1 is a sketch showing the three different environmental regimes encountered by the Moon in its orbit around the Earth: (1) the freely-streaming solar wind; (2) the magnetosheath, which consists of solar wind in a generally compressed and turbulent state produced by its interaction with the Earth's magnetic field; and (3) the geomagnetic tail, which is the downstream extension of the cavity formed in the flow of the solar wind by the Earth's magnetic field. Figure 2 shows three sections of the record obtained with the Apollo 15 subsatellite in orbit around the Moon. One section is from each of these three regions in near-Earth space. These records are typical in that the magnetosheath data are by far the most variable, the data from

the geomagnetic tail are the least variable, and those from the free-streaming solar wind are intermediate in variability.

Since the remanent magnetic field of the Moon is relatively weak, we have to date used only those subsatellite magnetometer data recorded while the Moon was in the geomagnetic tail for our studies of the remanent magnetic field of the Moon. At such times the Moon is immersed in a geomagnetic tail field which is of the order of 10 nT in strength, but, as shown in figure 2, is relatively constant.

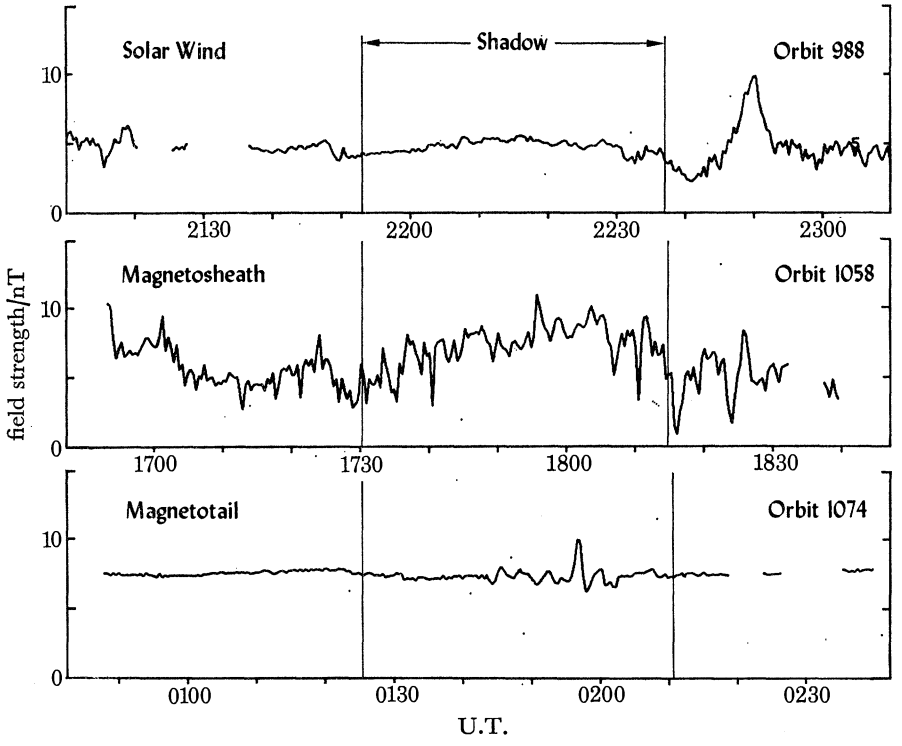

FIGURE 2. Magnetic field strength against time during three orbital revolutions of the Apollo 15 subsatellite around the Moon. The first record (top) was obtained while the Moon was in the solar wind, the second while it was in the magneto-sheath and the third while it was in the geomagnetic tail (after Schubert & Lichtenstein 1974).

With the data obtained during the Moon's traversals of the geomagnetic tail, we have attempted to measure the dipole moment of the Moon and to map the distribution of smaller-scale remanent fields. The Apollo subsatellite flew over 50 % of the lunar surface, but only about 14 % of the surface was overflown while the Moon was in the geomagnetic tail and the tail field was sufficiently constant for this analysis. Further, almost all of the measurements made at altitudes less than 80 km were taken over the far side of the Moon.

Figures 3 and 4 are plots of the radial component of the field strength against altitude for Apollos 15 and 16, respectively (Russell *et al.* 1975*a*). The data plotted are averages by longitudinal quadrant. The positive (outward) and negative (inward) fields are plotted separately.

From these figures, it is clear that the altitude dependence of the field increases rapidly with decreasing altitude. Thus, the field strength averages about 1 nT at 20 km. The aforementioned paucity of low-altitude coverage over the near side is also apparent.

Contour maps of the remanent field have been constructed from the measurements taken with both subsatellites in the altitude range 60–170 km. Figures 5–8 are, respectively, maps of the radial, east, and north components and the strength of the total field, for the same limited range of selenographic longitude.

These contour maps of the field are the result of a continuing effort to characterize accurately the Moon's remanent field. From internal consistency checks based on the requirement that the divergence of the field be zero, we believe that these maps are accurate to the 1/8 nT indicated by our selection of contour levels. A more extensive description of these maps and their construction has been provided by Russell *et al.* (1975*a*).

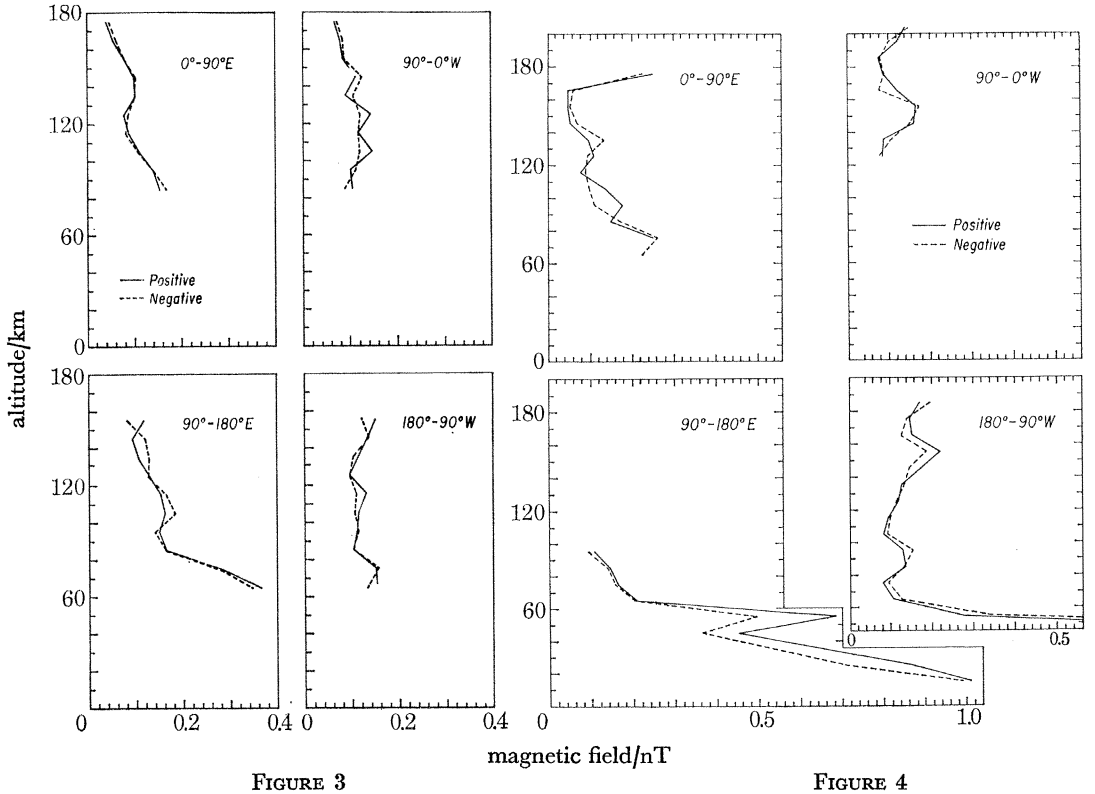

FIGURE 3

FIGURE 4

FIGURE 3. Average intensity of the radial component of the magnetic field versus altitude for the four quadrants of selenographic longitude. Positive (radially outward) and negative fields are averaged separately. The data were taken with the Apollo 15 subsatellite magnetometer (after Russell *et al.* 1975*a*).

FIGURE 4. As figure 3. These data were taken with Apollo 16 subsatellite magnetometer.

In figures 9–11, the radial, eastward and northward components, respectively, measured with the magnetometer on board Apollo 16, are compared at higher (60–170 km) and lower (10–60 km) altitudes.

This comparison lends additional support to our conclusion that the higher altitude maps are accurate to 1/8 nT, since all of the features in the higher altitude maps are apparent at greater intensities in the lower altitude maps. Further, the relatively high intensities and small scale sizes indicated in the maps derived from the lower altitude data suggest that the strength and variability of the magnetic field components in the vicinity of the Apollo 16 landing site are typical of a large part of the lunar surface.

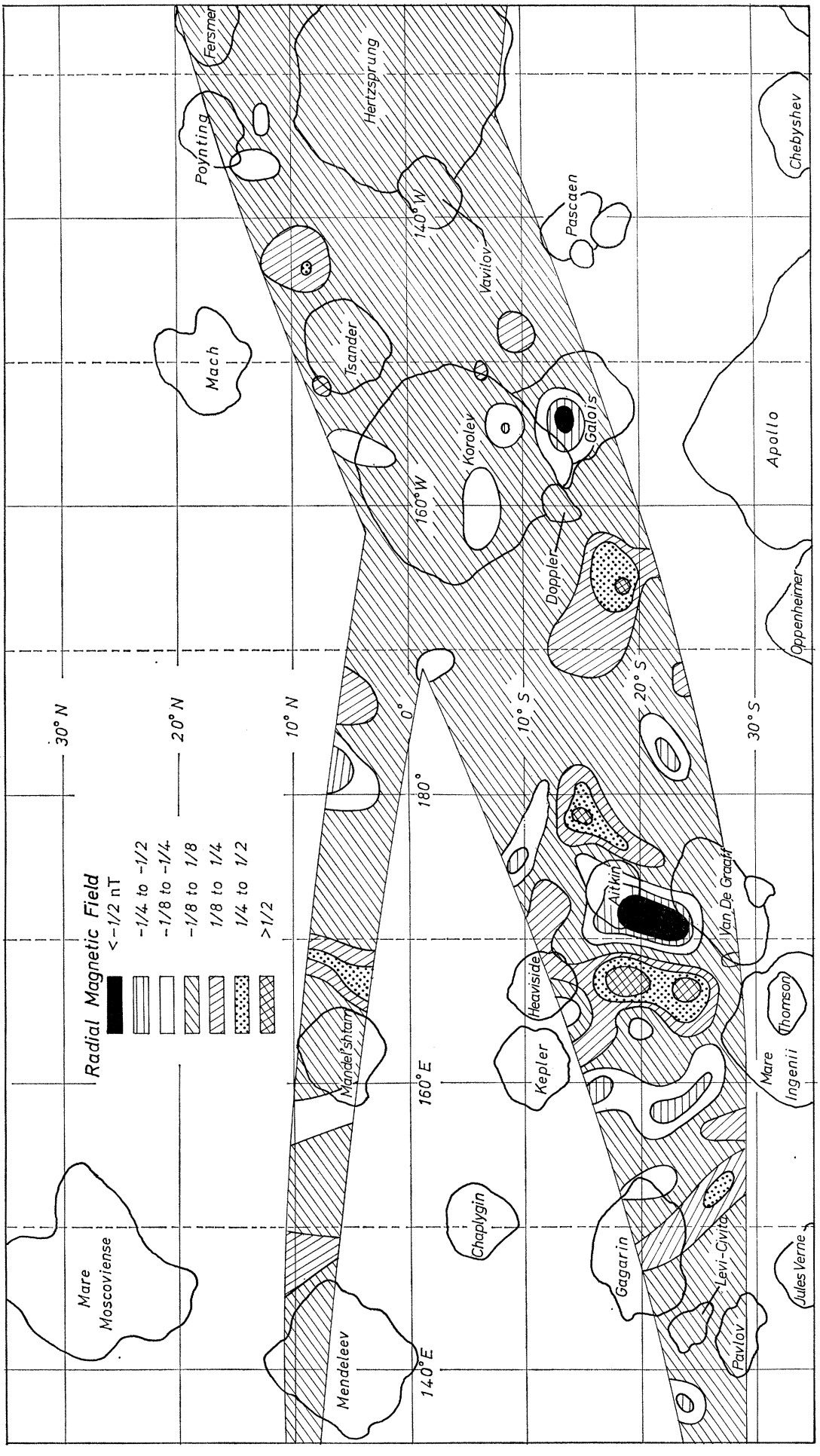

FIGURE 5. Contour map of the intensity of the radial component of the Moon's remanent magnetic field (after Russell *et al.* 1975*a*).

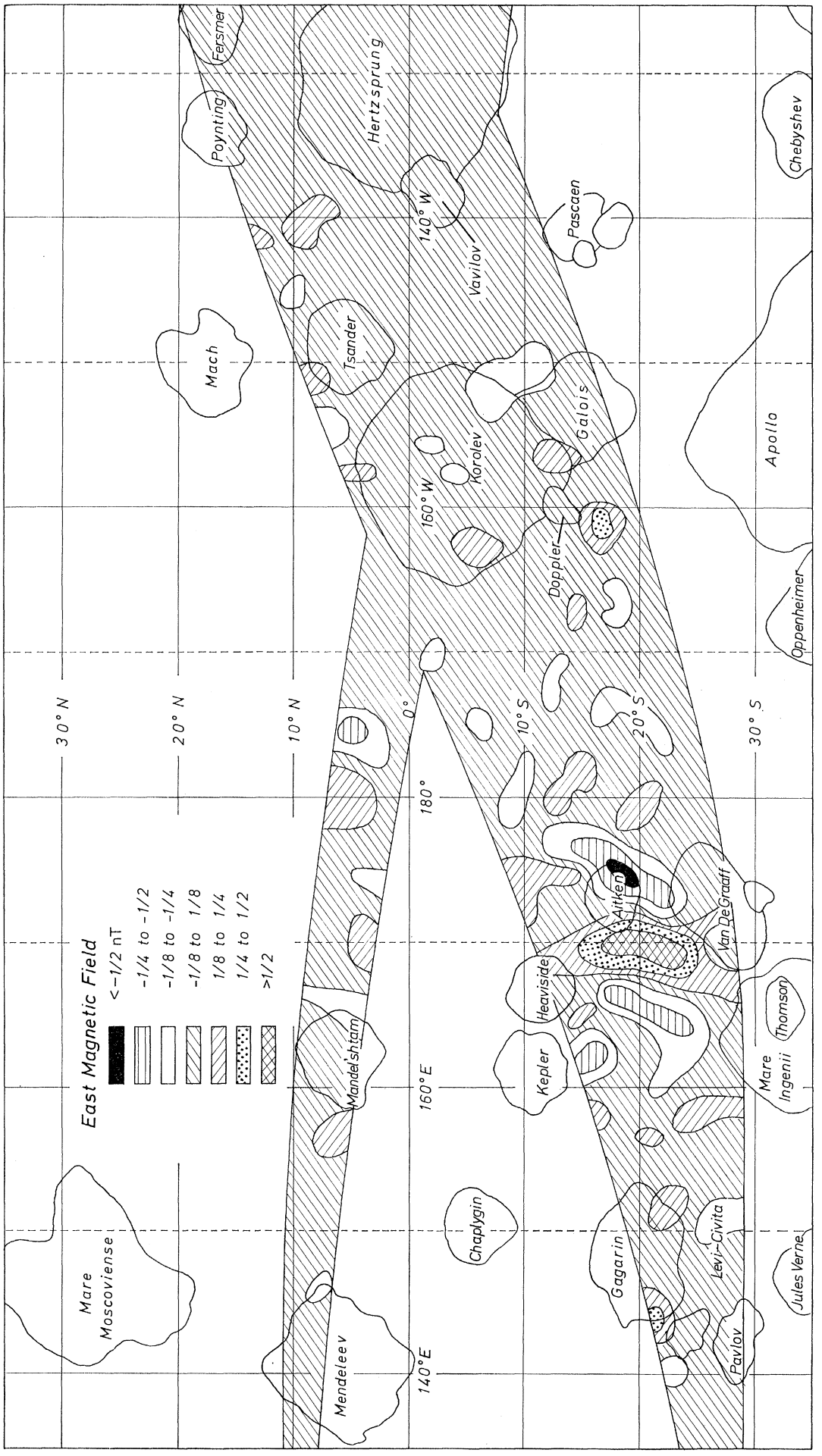

FIGURE 6. As figure 5 for the eastward component.

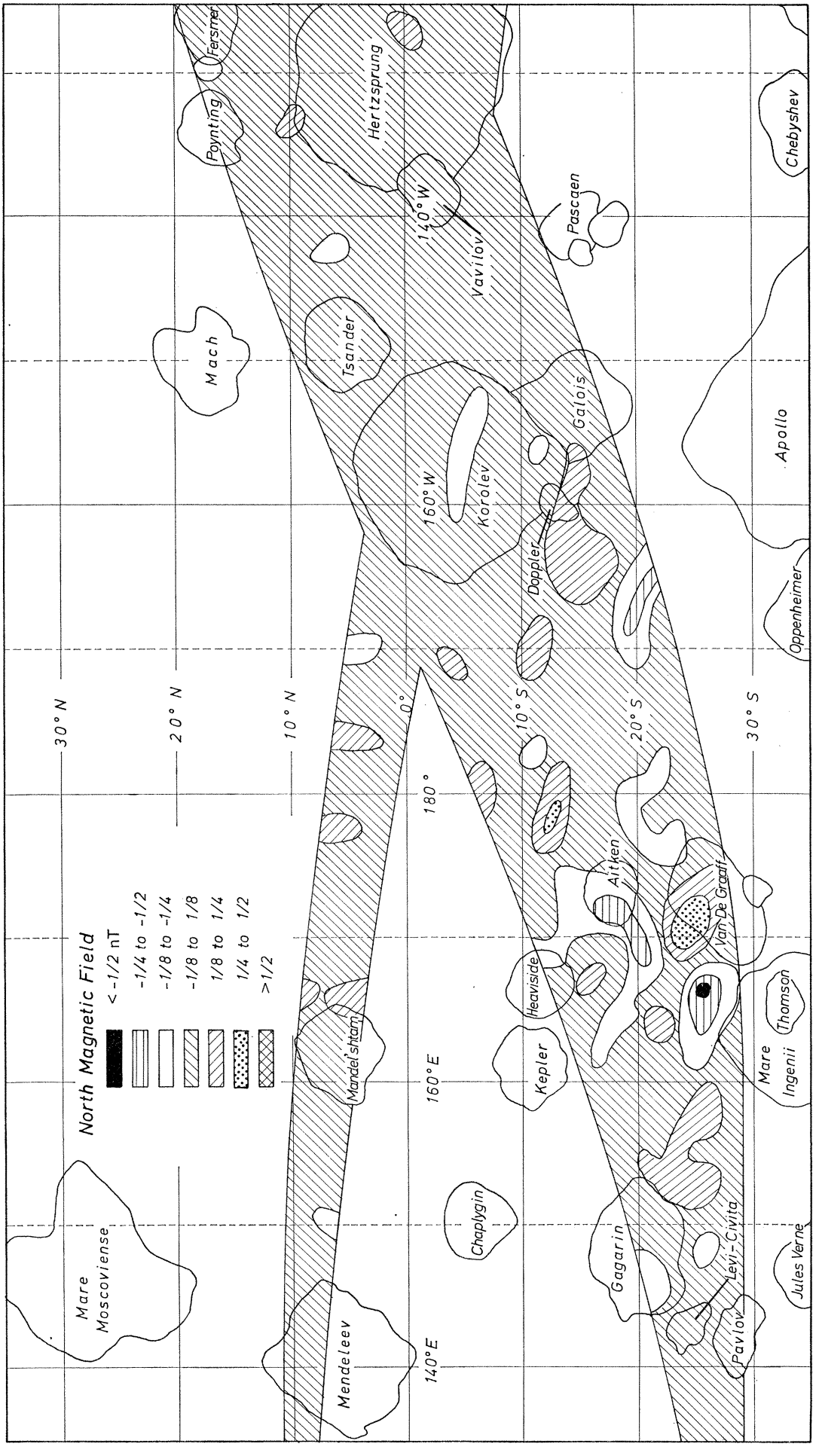

FIGURE 7. As figure 5 for the northward component.

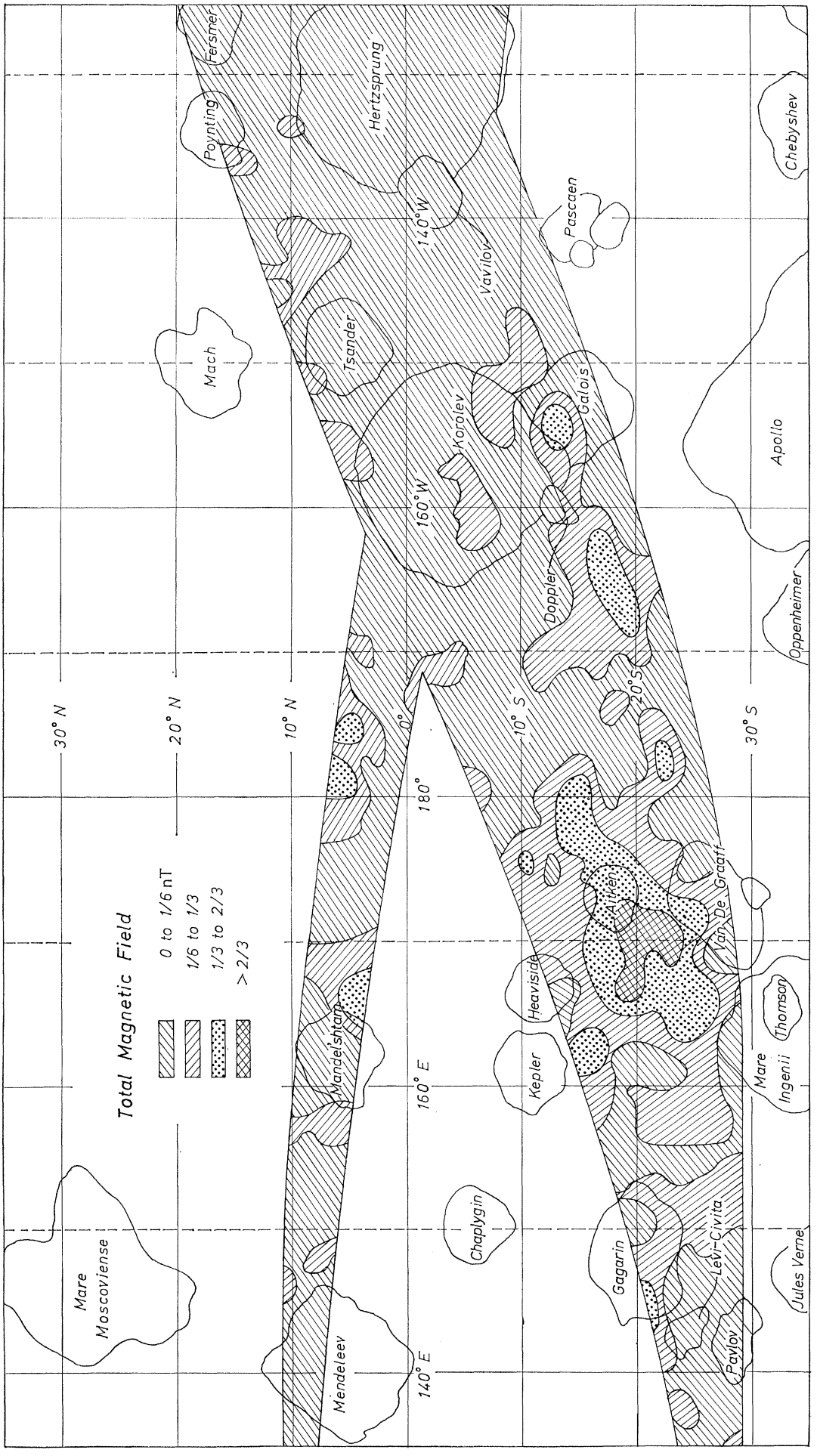

FIGURE 8. As figure 5 for the magnitude of the vector field.

PHILOSOPHICAL TRANSACTIONS OF THE ROYAL SOCIETY A MATHEMATICAL, PHYSICAL & ENGINEERING SCIENCES

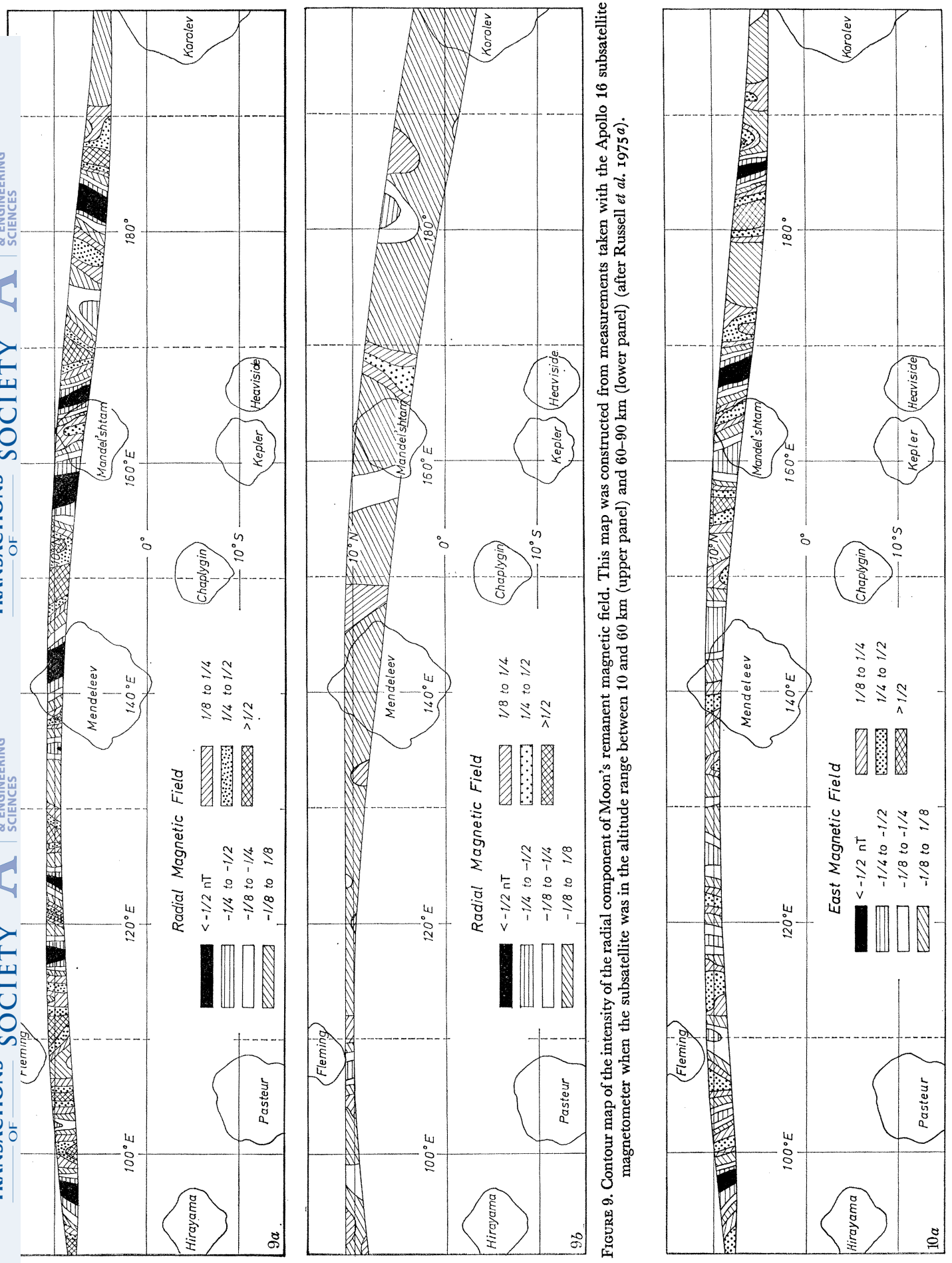

FIGURE 9. Contour map of the intensity of the radial component of Moon's remanent magnetic field. This map was constructed from measurements taken with the Apollo 16 subsatellite magnetometer when the subsatellite was in the altitude range between 10 and 60 km (upper panel) and 60–90 km (lower panel) (after Russell *et al.* 1975*a*).

FIGURE 10*a*. Same as figure 9 for the eastward component.

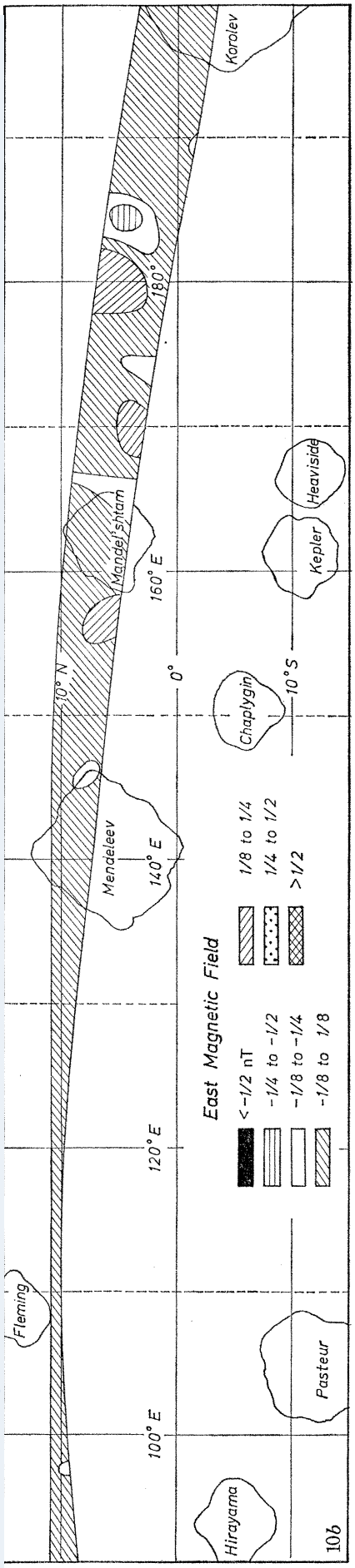

FIGURE 10*b*. Same as figure 9 for the eastward component.

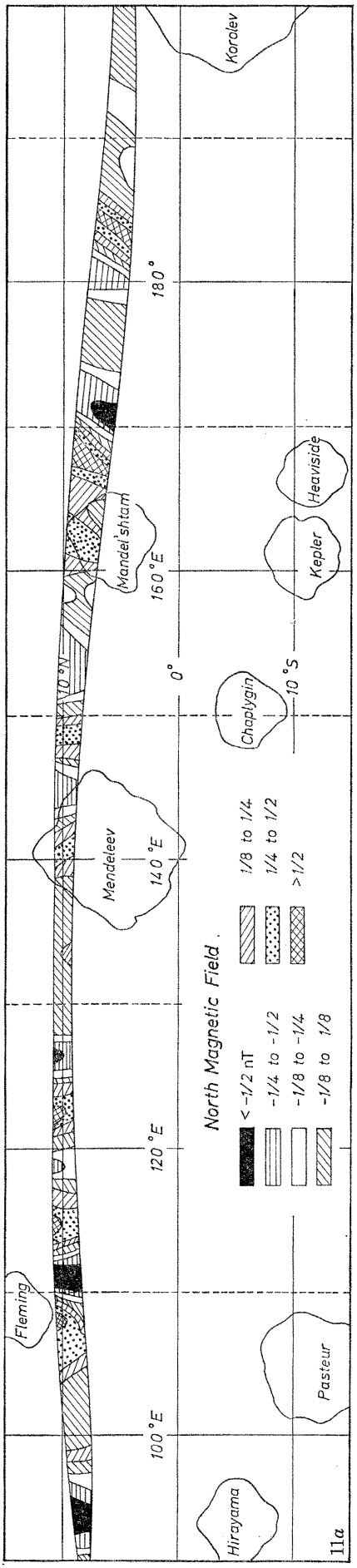

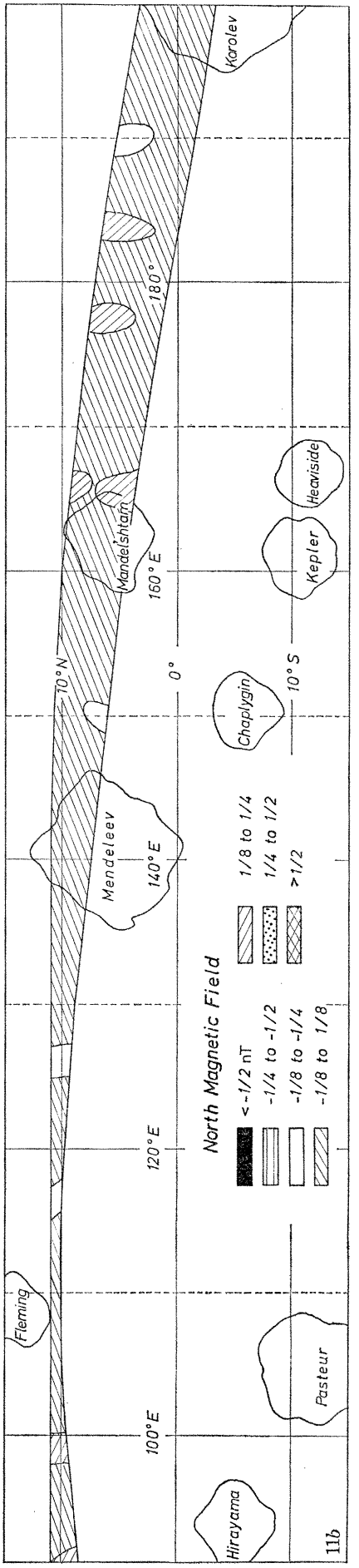

FIGURE 11. Same as figure 9 for the northward component.

We have also attempted to fit the subsatellite measurements of the Moon's remanent field with models of various types. One of our efforts has been to determine the characteristics of the dipole moment of the relatively strong source in the Van de Graaff region, a source which is apparent in figures 11–13. In our latest calculation (Russell *et al.* 1975*a*), we used 100 vector measurements recorded at altitudes below 100 km and within a longitude range between 168.5 and 174.0° E. For this data set, our best fit dipole moment $\boldsymbol{M}$, obtained by using a Kalman filtering technique (Ioannidis 1975), has components M_z (along the Moon's axis of rotation), $+0.7\times10^{16}\,\Gamma\,\mathrm{cm}^3$; $M_y = 0.1\times10^{16}$; and M_x (towards Earth), $+1.7\times10^{16}$; so that $|\boldsymbol{M}| = 1.8\times10^{16}$. The location of this dipole source is latitude 20.5° S, longitude 172.8° E, and depth 94 km.

This effective depth is approximately that expected for a near surface field source consisting of a uniformly magnetized disk with a radius of 94 km (Runcorn 1975*a*).

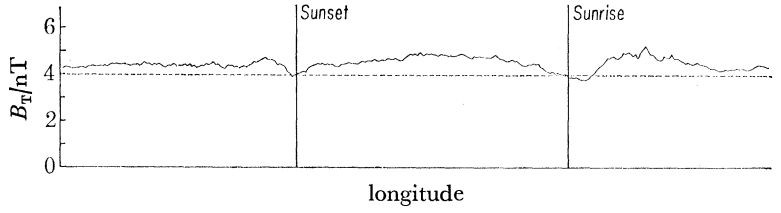

FIGURE 12. Average magnetic field versus longitude from subsatellite point for 121 orbital periods by Apollo 15 subsatellite while the Moon was in the solar wind. (The specific field component plotted here is that transverse to the spin axis of the subsatellite) (after Coleman *et al.* 1972*b*).

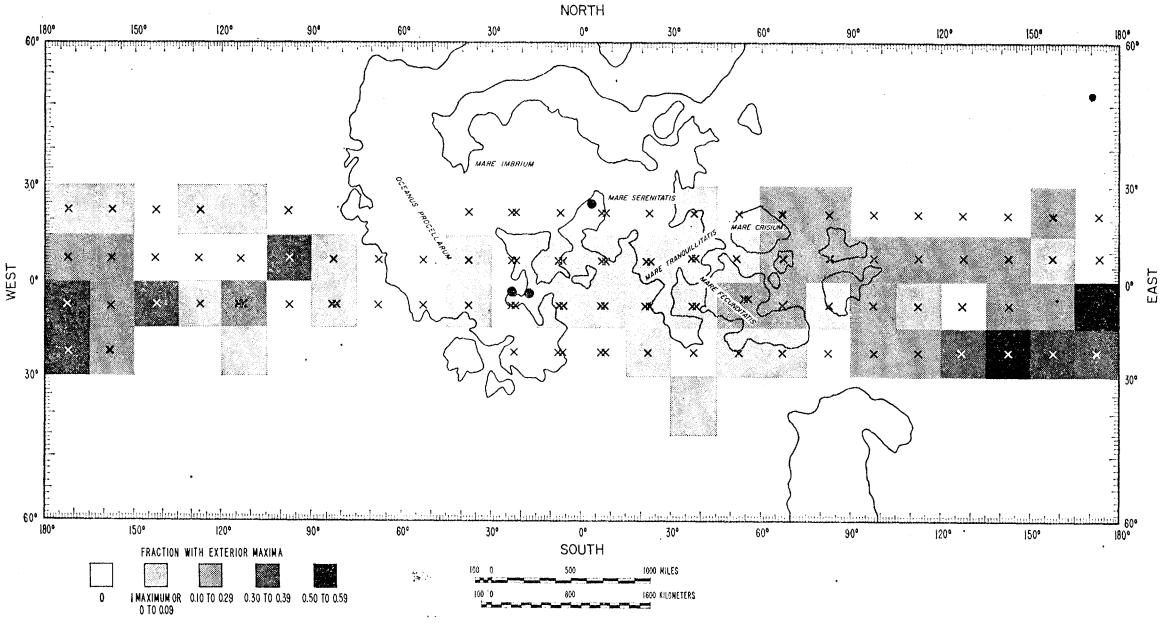

FIGURE 13. Mercator map of the Moon showing the concentration of the assumed sources of limb disturbances. The shading in the 15° × 15° areas indicates the fraction of the time that the characteristic signature was observed at Explorer 35 when it was at the lunar limbs and thus exposed to the grazing incidence of the solar wind. One cross indicates that it was so oriented between 11 and 20 times, two crosses indicate that the region was so oriented more than 20 times during the study. The data show positions of the sites of Apollos 12, 14, and 15 (after Sonett & Mihalov 1972).

PHILOSOPHICAL TRANSACTIONS OF THE ROYAL SOCIETY A MATHEMATICAL, PHYSICAL & ENGINEERING SCIENCES

We have also used the data recorded in the geomagnetic tail to estimate the dipole moment of the Moon's permanent magnetic field (Russell *et al.* 1975*b*). The results of these estimates are shown in table 2. In obtaining these estimates, the data from each subsatellite were used to measure the component of $\boldsymbol{M}$ in the orbital plane. This approach was employed in order to minimize the possibility that the relatively strong tail field, even though fairly constant, would introduce a bias in the results, especially in the results on the component perpendicular to the orbit plane. Since the subsatellite orbits were inclined to one another by about 40°, the components in the two orbit planes can, in principle, be combined to yield an estimate of the three components of the dipole moment, thus eliminating the need to use estimates from either spacecraft of the components perpendicular to their respective orbital planes.

TABLE 2. PERMANENT MAGNETIC DIPOLE MOMENT

	Apollo 15		Apollo 16	
	i	*j*	*k*	*l*
radial	$2.58 \times 10^{18} \Gamma$ cm^3	$1.04 \times 10^{18} \Gamma$ cm^3	$1.64 \times 10^{18} \Gamma$ cm^3	$-5.38 \times 10^{18} \Gamma$ cm^3
tangential	−0.20	0.05	1.82	−7.24
average	1.19	0.54	1.73	−6.31
difference	1.39	0.50	−0.09	0.93
perpendicular	−2.81	1.44	−12.7	−0.50
error estimate	0.9	0.9	3.8	3.8

In table 2, for the Apollo 15 data, *i* is the component in the orbit plane at 0° selenographic longitude and *j* is the component in the orbit plane 90° to the east. For the Apollo 16 data, these components are *k* and *l*, respectively. For each orbit, by using the radial component of the field and, separately, the component tangential to the orbit, one can obtain independent estimates of the components of the projection of $\boldsymbol{M}$ in the corresponding orbital plane. These estimates are shown separately for the two subsatellites. Estimates for the component perpendicular to the plane of each orbit are also shown, to provide a qualitative basis for error estimates.

The combined results give the estimate for $\boldsymbol{M}$ shown at the bottom of the table. In this case, the dipole moment is inclined at 34° to the axis of the Moon, and the magnitude of the dipole moment is approximately $1.1 \times 10^{19} \Gamma$ cm^3.

In these estimates, the internal consistency is rather unsatisfactory, i.e. the estimates of the in-plane component of $\boldsymbol{M}$ differ considerably for the two spacecraft. Even for the same spacecraft the estimates for this component differ significantly depending on whether the radial or tangential field was used. Thus, we have suggested that this calculated value be treated as an upper limit to the Moon's dipole moment.

INDIRECT MEASUREMENTS OF THE MOON'S REMANENT FIELD

Colburn *et al.* (1967), using a magnetometer on board Explorer 35, found that the Moon produces a characteristic disturbance in the magnetic field of the solar wind. The essential features of this disturbance are interpreted as being consequences of the fact that the solar wind hits the surface of the Moon, thus creating a void immediately behind the Moon. The structure of the solar wind magnetic field in the vicinity of the Moon clearly shows the presence of the downstream void as well as a characteristic variation across the boundary of the void. This field

pattern is evident in figure 12 (Coleman *et al.* 1972*b*), which shows the average magnetic field for 121 orbits of the Apollo 15 subsatellite, taken while the Moon was in the solar wind.

The Explorer 35 team also found that the pattern of the solar wind magnetic field frequently differed in a systematic fashion from the average pattern suggested by figure 12, and that the major departures were in the regions near the boundary of the downstream cavity. They showed that these departures of this disturbance are interpreted as being consequences of the fact that the solar wind hits the surface of the Moon, thus creating a void immediately behind the Moon. The structure of the solar wind magnetic field in the vicinity of the Moon clearly shows the presence of the downstream void as well as a characteristic variation across the boundary of the void.

At the much lower altitudes of the Apollo subsatellites, the magnetic effects associated with these limb disturbances are relatively substantial. An example is shown in figure 14, which the reader may compare to the 'average' pattern shown in figure 12.

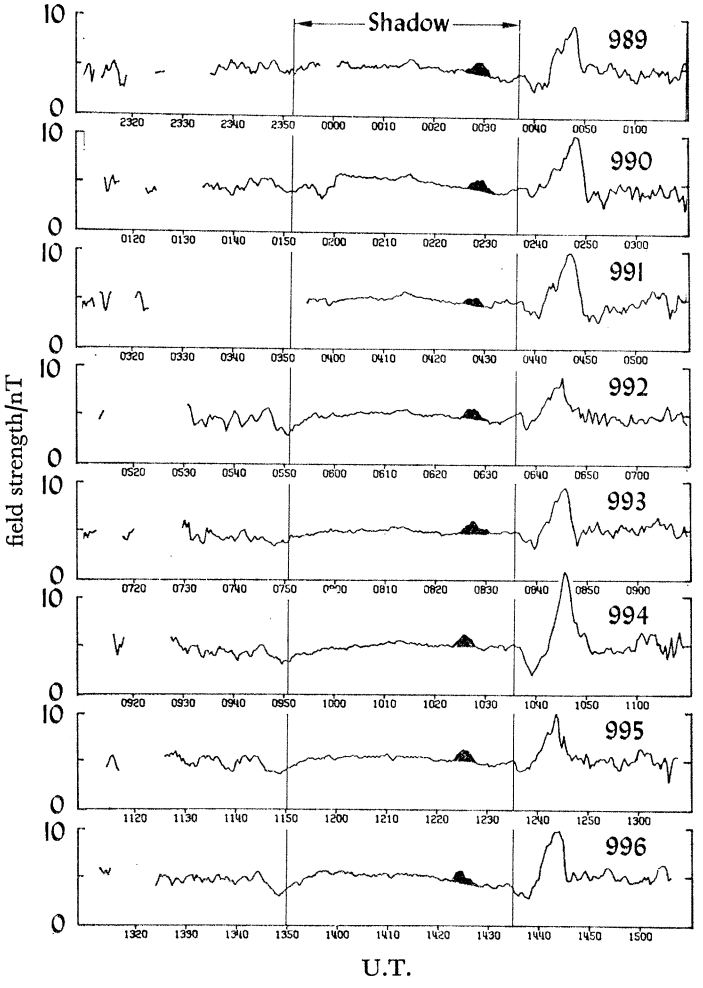

FIGURE 14. Magnitude of the magnetic field measured with the Apollo 15 subsatellite on eight consecutive subsatellite orbits during which the Moon was in the solar wind. The interval marked 'shadows' is that during which the subsatellite is in the shadow of the Moon. The large evolving feature on the right hand side of the figure is associated with a limb disturbance. The shaded feature within the 'shadow' interval is apparently produced by the remanent field (after Schubert & Lichtenstein 1974).

PHILOSOPHICAL TRANSACTIONS OF THE ROYAL SOCIETY A MATHEMATICAL, PHYSICAL & ENGINEERING SCIENCES

In figure 15 is shown the distribution of the regions associated with the disturbances that were detected with the Apollo subsatellites (Schubert & Lichtenstein 1974). In comparing the results from Explorer 35 to those from the closer and therefore 'more sensitive' subsatellites, it was found that wherever the coverage overlapped, nearly all of the sources detected with Explorer 35 were detected, among others, with the subsatellites.

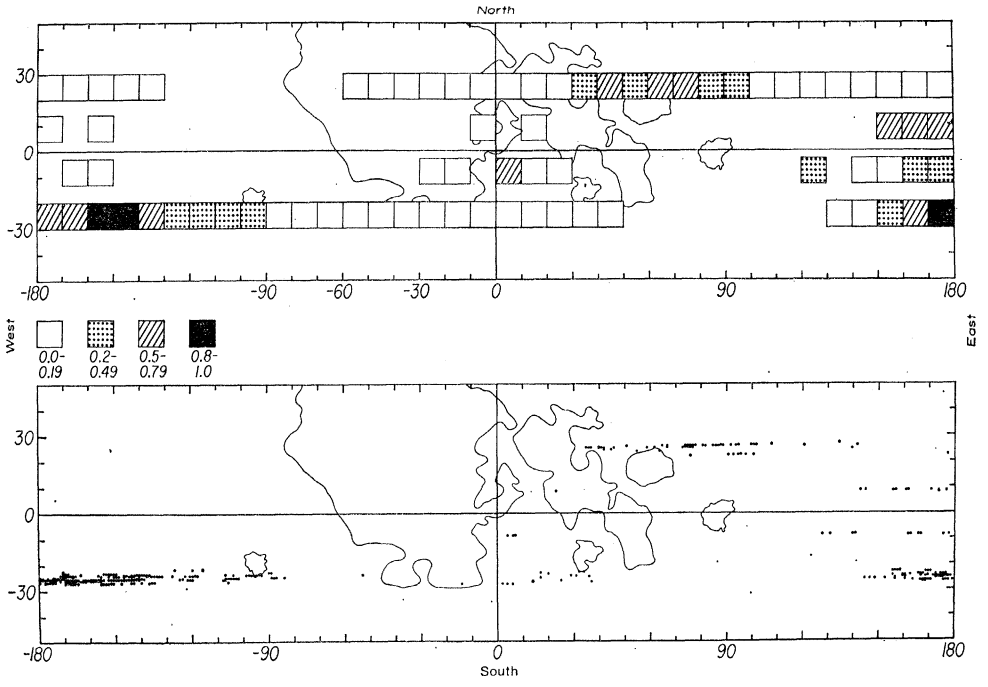

FIGURE 15. Regions associated with limb disturbances detected with the Apollo 15 and 16 subsatellites. The upper panel is a map of the normalized occurrence rate for areas 10° × 10°. The lower panel shows the distribution of the estimated locations of the disturbance sources (after Schubert & Lichtenstein 1974).

Further, although only about 8 % of the Moon's surface was covered in the investigation of the limb disturbances using the subsatellite data, there was some overlap of the resulting remanent field maps and the 'limb disturbance source' map of figure 15. In the regions of overlap, the regions associated with the larger limb disturbances are also characterized by relatively strong fields. These results thus favour the suggestion that the measurements of the properties of these limb disturbances provide indirect measurements of the remanent magnetic field on the lunar surface.

As might be expected, from the foregoing the Van de Graaff region, which exhibits the strongest fields detected from orbit to date also produces one of the larger-scale or larger amplitude limb disturbances. However, as shown in figure 16, it does not produce the greatest of the disturbances recorded to date (Russell & Lichtenstein 1975). Thus, to the extent that the dimension and magnitude of a limb shock may be associated with the scale size and intensity of the field source, there is evidence that there are regions on the Moon with stronger magnetic sources than the Van de Graaff region. One such region is located at roughly the latitude of Van de Graaff and approximately at 150° W longitude.

The other indirect method for measuring the Moon's remanent field involves the scattering of energetic electrons by the field. Studies of the patterns of these scattered electrons by

Anderson and his colleagues (McCoy *et al.* 1974) using measurements obtained with instruments on board the two Apollo subsatellites have proven to be remarkably good indicators of the fine structure of the surface magnetic field. Work with this method promises to extend our knowledge of the surface field considerably.

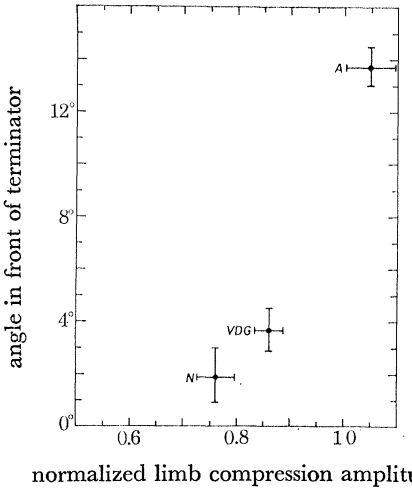

FIGURE 16. The average angle ahead of the terminator at which peak compression is observed against average strength of limb compression for three strongest proven regions. Error bars represent the probable error of the mean (after Russell & Lichtenstein 1975).

SUMMARY OF OBSERVATIONS

The results discussed in the foregoing may be summarized as follows:

(1) Magnetization of the intensity and spatial variability indicated by the surface traverse at the Apollo 16 site is evidently characteristic of a significant fraction of the lunar surface, at least at the lower latitudes covered by the Apollo 16 subsatellites.

(2) Scale sizes of the field sources range from 1 to at least 100 km.

(3) The source near Van de Graaff is estimated to have a scale size on the order of 100 km. It is either at least 25 km in scale size or its mean magnetization is greater than any of the lunar samples examined to date.

(4) There are regions on the Moon that exhibit magnetic sources stronger than that in the vicinity of Van de Graaff.

(5) Taken together, the information on limb disturbances and the direct measurements of the remanent field indicate that the magnetic fields on the far side of the Moon are stronger and more variable than those on the near side.

(6) The strong correlation of limb disturbance occurrence with the presence of remanent magnetic field sources in the lower-latitude terminator region in combination with the apparent lack of disturbances from sources at higher latitudes included in the Explorer 35 data (Sonett & Mihalov 1972) suggests a significant latitude dependence in the Moon's remanent magnetic field. The further investigation of this possibility is a prime candidate for the proposed lunar polar orbiter mission.

Discussion

The measured gradients of the remanent field can be used to place limits on the magnetizations and dimensions of the field sources. The maximum gradient in the field strength measured to date is that corresponding to the 122 nT difference between the 235 nT field of the Apollo 16 station magnetometer and the 113 nT field at the last position of the lunar rover (final l.r.v. site), as shown in table 1. These two positions were separated by only 0.4 km. (Further details of the remanent field measurements at the Apollo sites are contained in Dyal *et al.* 1974.) The maximum radius of a buried, uniformly magnetized spherical source that can produce this intensity gradient is very roughly 0.5 km and the minimum magnetization corresponding to 235 nT is roughly $6 \times 10^{-4}\ \Gamma\ \mathrm{cm^3/cm^3}$, or about $2 \times 10^{-4}\ \Gamma\ \mathrm{cm^3/g}$, well within the range 10^{-7}–$10^{-3}\ \Gamma\ \mathrm{cm^3/g}$ of the Apollo samples measured to date. (The sample work has recently been reviewed by Fuller (1974).)

The strongest larger-scale source surveyed directly is that in the vicinity of Van de Graaff. As discussed earlier, the indicated maximum radius is approximately 90 km and its dipole moment is about $2 \times 10^{16}\ \mathrm{G\ cm^3}$. The minimum magnetization is then roughly $3 \times 10^{-5}\ \mathrm{G\ cm^3/cm^3}$, or $10^{-5}\ \mathrm{G\ cm^3/g}$, again well within the range exhibited by the lunar samples. Thus, from the measurements obtained to date, it would appear that the magnetic fields on the Moon can be accounted for in terms of a distribution of materials magnetized to the levels measured in the Apollo lunar samples.

Next, we turn to a consideration of the near side–far side asymmetry. The satellite observations indicate that the far side is more strongly magnetized on the average than is the near side. Further, the intensity of magnetization is more variable. An obvious difference between the two regions is the existence of the maria as a dominant feature on the near side, and the fields over the maria appear to be particularly weak and uniform. Four possible explanations for the relative regularity of the mare fields suggest themselves. First, the crustal material on the near side may simply be less strongly magnetized than on the far side. Secondly, the basins underlying the flooded maria may be smoother than the basins of comparable dimensions on the far side. Thirdly, the flooding may have somehow changed the levels of magnetization of the crustal material beneath the flooded regions. Finally, the mare basalts may have somehow modified the magnetic field significantly by virtue of their own magnetization.

Figure 13, from Sonett & Mihalov (1972), shows that there are sources of limb effects in the highlands between the near side maria. A similar conclusion may be drawn from the satellite data of figure 15. This fact suggests that the near side crustal material, as it existed before the basin formation, was appreciably magnetized. Thus, the first possibility seems not to be the obvious answer, although the evidence for near side–far side asymmetry in crustal thickness (Kaula *et al.* 1974) and the possible effects of this asymmetry in a magnetized crust have not been taken into account here. Any shielding by the mare basalts seems unlikely. Demagnetization by heating during the flooding would seem to be more or less likely depending upon whether the flooding was a single event or episodic.

However, the near side mare basins are believed to be considerably younger than the basins of comparable size on the far side. Thus, one might expect that the basins underlying the flooded regions are smoother than the older unfilled basins on the far side and that the remanent fields from the crustal material underlying the near side maria would be more regular.

On the matter of the origin and history of the field responsible for the remanent magnetization

of the Moon, we have another set of results to consider. Based on laboratory studies of lunar samples by Collinson *et al.* (1973), Gose *et al.* (1973) and Stephenson & Collinson (1974), the intensity of the magnetizing field has been estimated to lie between 2 μT and 1.2 G (0.12 mT). Along with these results we have our estimates of the present dipole moment of the Moon and of the dipolar component of the field in the Van de Graaff region, and the evidence from studies of limb disturbances for a latitude dependence in the properties of the remanent field. With these data it is possible to test some simple models.

Runcorn (1975*b*) has pointed out the differences between remanent fields that would be acquired by a uniformly magnetizable spherical shell under the influence of an internal dipolar magnetic field in the two limiting cases in which the material is either weakly or strongly permeable. In the former case, i.e. in the case in which there is essentially no shielding by the outer shell, Runcorn (1975*a*) has shown that the remanent field of the shell is zero everywhere outside the shell. In the latter case it is, of course, a non-zero field that is dipolar in its lowest order. On the other hand, if such a shell is subjected to an external, uniform magnetic field, the remanent field, after the magnetizing field has decreased to zero, will be dipolar in both the weakly and strongly permeable limits.

The situation of interest is one in which these magnetized shells are modified by a redistribution of the material of which they are composed. At the simplest situation, we have considered cases in which the geometries of such shells are changed mechanically by processes such as impacts, while the magnetization of the material remains the same (Coleman 1975). Some fairly simple geometries are instructive. Consider, for example, holes punched in such shells. For three of the four cases; i.e. for both the weakly and strongly permeable shells magnetized by an external uniform field as well as for the strongly permeable shell magnetized by an internal dipolar field, a hole anywhere in the shell will reduce the magnitude of the remanent dipole moment but will not change its direction. However, for the weakly permeable spherical shell magnetized originally by an internal dipole, holes in the shell will, in general, produce a non-zero external remanent field with a dipole moment that is neither parallel nor antiparallel to that of the internal field that originally magnetized the shell. For example, suppose the magnetizing dipole, now vanished, was of moment $\boldsymbol{M}$ parallel to the polar axis. A crater centred at the pole produces an external field with a dipole moment opposite $\boldsymbol{M}$. A crater centred on the equator produces an external field with a dipole moment parallel to $\boldsymbol{M}$. A crater centred at roughly latitude 36° produces an external field with a dipole moment transverse to $\boldsymbol{M}$ and the polar axis. Thus, as the crater centre is shifted from the pole through 36° latitude to the equator at a constant longitude, the orientation of the dipole moment of the resulting external field rotates from that antiparallel to $\boldsymbol{M}$ through that perpendicular to $\boldsymbol{M}$ to that parallel to $\boldsymbol{M}$.

For a roughly symmetrical distribution of holes, the external field exhibits a fairly simple dependence upon latitude, with the maximum transverse component at latitudes near 36°. Since the component transverse to the Moon's axis is at the limb, roughly parallel or antiparallel to the average interplanetary magnetic field, this variation of orientation with latitude might account for a latitude dependence of the distribution of limb disturbance source, such as that suggested by Sonett & Mihalov (1972).

Here we have considered only situations in which the remanent magnetization is symmetrical about the Moon's rotational axis. Thus, if the magnetizing source was an internal dipole which reversed as has the Earth's, the net magnetization would be more or less aligned along the spin axis because reversals occur in times that are short compared with the duration of the periods

PHILOSOPHICAL TRANSACTIONS OF THE ROYAL SOCIETY A MATHEMATICAL, PHYSICAL & ENGINEERING SCIENCES

during which the field has one polarity or the other. Also, a uniform magnetizing field impressed on a rotating body can produce magnetization only parallel to the spin axis.

Of course, these very simple models are no more than suggestive. We have modelled the effects for the case in which all of the material excavated from the holes is either removed from the vicinity of the Moon or oriented randomly so that it contributes nothing to the external field. Thus, we have not considered the effects of uplift, folding, and the non-random distribution and orientation of any magnetized ejecta.

Valuable discussions with F. El Baz, A. Stephenson and S. K. Runcorn, F.R.S. are gratefully acknowledged. This work was supported in part by the National Aeronautics and Space Administration under research grant NGR 05-007-351.

References (Coleman & Russell)

Colburn, D. S., Currie, R. G., Mihalov, J. D. & Sonett, C. P. 1967 *Science, N.Y.* **158**, 1040–1042.
Coleman, P. J., Jr. 1975 In preparation.
Coleman, P. J., Jr, Schubert, G., Russell, C. T. & Sharp, L. R. 1972*a* *Moon* **4**, 419–429.
Coleman, P. J., Jr, Lichtenstein, B. R., Russell, C. T., Sharp, L. R. & Schubert, G. 1972*b* *Apollo 16 Prelim. Sci. Rep.*, NASA Publ. SP-315, 23-1-23-13.
Collinson, D. W., Stephenson, A. & Runcorn, S. K. 1973 *Proc. 4th Lunar Sci. Conf.*, pp. 2963–2976.
Dyal, P., Parkin, C. W., Synder, C. W. & Clay, D. R. 1972 *Nature, Lond.* **236**, 381–385.
Dyal, P., Parkin, C. W. & Daily, W. D. 1973 *Proc. 4th Lunar Sci. Conf.*, pp. 2925–2945.
Dyal, P., Parkin, G. W. & Daily, W. D. 1974 *Rev. Geophys. Space Phys.* **12**, 568–591.
Fuller, M. 1974 *Rev. Geophys. Space Phys.* **12**, 23–70.
Gose, W. A., Strangway, D. W. & Pearce, G. W. 1973 *Moon* **7**, 198–201.
Ioannidis, G. 1975 *IGPP Publ.* 1414, UCLA.
Kaula, W. M., Schubert, G., Lingenfelter, R. E., Sjogren, W. L. & Wollenhaupt, W. R. 1974 *Lunar Sci.* **5**, 399–401.
McCoy, J. E., Anderson, K. A., Lin, R. P., Howe, H. C. & McGuire, R. E. 1974 *Proc. Lunar Inst. Conf.*, Lake Geneva, Wisc.
Runcorn, S. K. 1975*a* *Phys. Earth Planet Int.* (In the press.)
Runcorn, S. K. 1975*b* *Nature, Lond.* **253**, 701–703.
Russell, C. T. & Lichtenstein, B. R. 1975 *J. geophys. Res.* (In the press.)
Russell, C. T., Coleman, P. J., Jr, Fleming, B. K., Hilburn, L., Ioannidis, G., Lichtenstein, B. R. & Schubert, G. 1975*a* *Proc. 6th Lunar Sci. Conf.* (In the press.)
Russell, C. T., Coleman, P. J., Jr. & Schubert, G. 1975*b* *Space Res.* **15** (in the press).
Schubert, G. & Lichtenstein, B. R. 1974 *Rev. Geophys. Space Phys.* **12**, 592–623.
Sonett, C. P. & Mihalov, J. D. 1972 *J. geophys. Res.* **77**, 588–603.
Stephenson, A. & Collinson, D. W. 1974 *Earth Planet Sci. Lett.* **23**, 220–228.

PHILOSOPHICAL TRANSACTIONS OF THE ROYAL SOCIETY A MATHEMATICAL, PHYSICAL & ENGINEERING SCIENCES

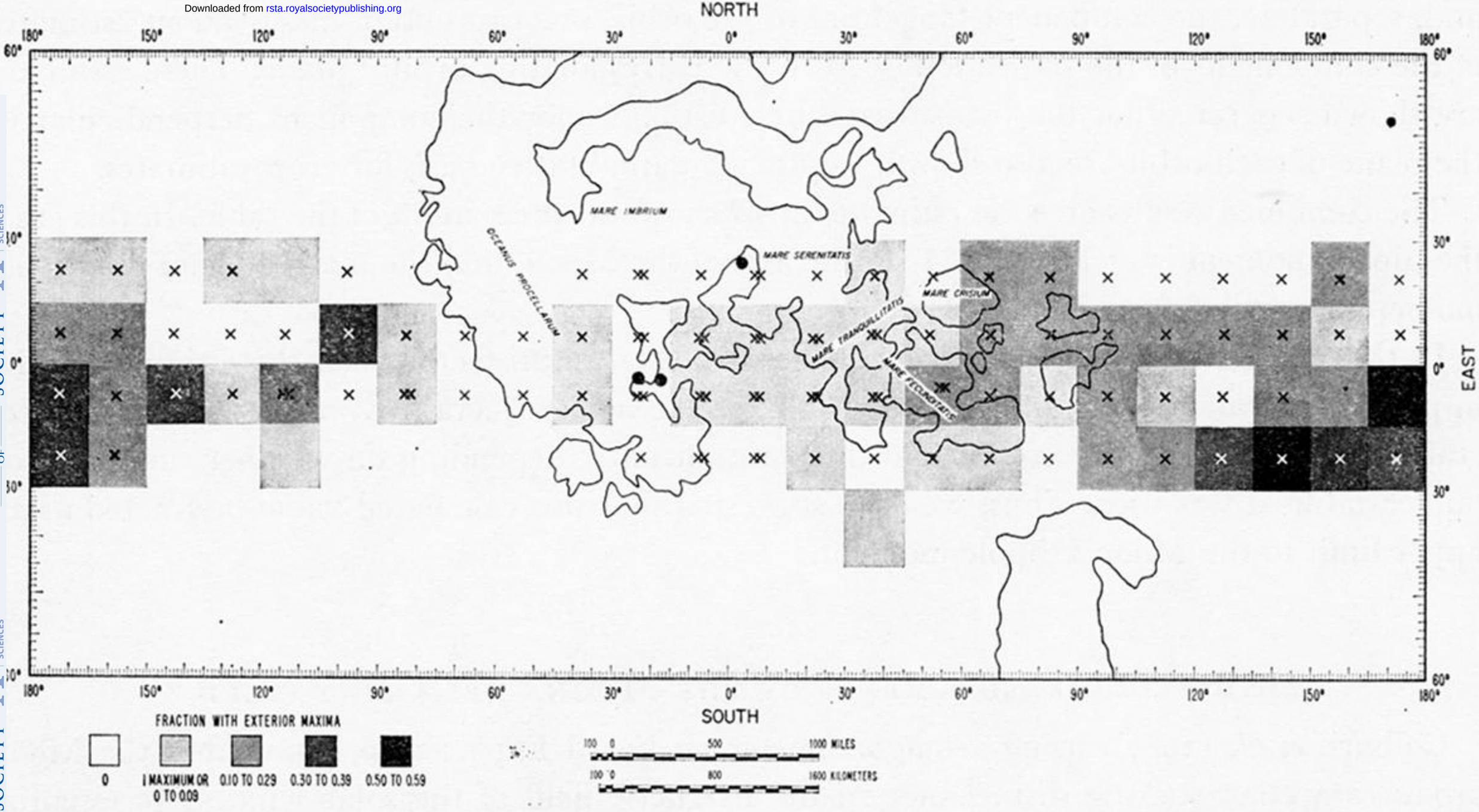

FIGURE 13. Mercator map of the Moon showing the concentration of the assumed sources of limb disturbances. The shading in the 15° × 15° areas indicates the fraction of the time that the characteristic signature was observed at Explorer 35 when it was at the lunar limbs and thus exposed to the grazing incidence of the solar wind. One cross indicates that it was so oriented between 11 and 20 times, two crosses indicate that the region was so oriented more than 20 times during the study. The data show positions of the sites of Apollos 12, 14, and 15 (after Sonett & Mihalov 1972).